AIAA JOURNAL
Vol. 48, No. 1, January 2010

Technical Notes

Experimental Study of Plasma Flow Control on Highly Swept Delta Wing

P. F. Zhang,* J. J. Wang,† L. H. Feng,‡ and G. B. Wang§
Beijing University of Aeronautics and Astronautics, 100191 Beijing, People's Republic of China

DOI: 10.2514/1.40274

I. Introduction

AERODYNAMIC flow control based on plasma actuators is now in expansion, because plasma actuators are fully electronic with no moving parts; they have an extremely fast response, very low mass, low input power, and the easy ability to simulate their effect in numerical flow solvers [1]. In particular, they are flexible, so that they can be formed to various shapes and located on the air vehicles with relative ease. There are no other known actuators that have such flexibility [2].

There are many different plasma actuators, including dielectric barrier discharge (DBD), direct current glow discharge, radio frequency glow discharge, and filamentary arc discharges. Suchomel et al. [3] provided an overview of different plasma generation technologies currently under investigation for aeronautical applications. The actuator used here is based on surface DBD. This new discharge was invented by Roth et al. and protected by a U.S. patent since 1995 [4]. The surface plasma has considerably influenced research on airflow control by plasmas, because the simplicity of its use allowed many researchers in aerodynamics to work on this subject (without necessarily being specialists in plasma generation [5]). Velocity measurements indicate that the primary result of the averaged plasma-induced body forces is the formation of a wall jet that imparts momentum to the fluid [1].

The plasma actuators for aerodynamic flow control can be applied for different purposes. Examples include boundary layer control [6], lift augmentation and separation control for airfoils [7,8], and control of the dynamic stall vortex on oscillating airfoils [9]. More recently, the plasma actuator has been demonstrated on application in three-dimensional vortical flow controls on delta wings and unmanned aerial vehicle (UAVs) [2,10–12].

Patel et al. [10] used the DBD plasma actuators for hingeless flow control over the 1303 unmanned combat air vehicle wing. Control was implemented at the wing leading edge to provide longitudinal control without the hinged control surfaces. Force balance results showed considerable changes in the lift characteristics of the wing for the plasma-controlled cases, when compared with the baseline cases. Compared with the conventional traditional trailing-edge devices, the plasma actuators were demonstrated to have a significant improvement in the control authority in the 15 to 35 deg angle-of-attack range, thereby extending the operational flight envelope of the wing. In addition to the lift modification, Nelson et al. [11] studied the plasma actuator to provide roll control at high angles of attack on a scaled 1303 UAV configuration. It was found to have excellent roll control capability, which was very responsive. Greenblatt et al. [2] investigated the DBD plasma actuator active control of a leading-edge vortex on a semispan delta wing at typical micro aerial vehicle Reynolds numbers. The plasma actuator produced a plasma-induced jet inward from the leading edge. The maximum C_L ($\alpha = 36$ deg) increased by 0.2 in the poststall region at the optimum reduced frequency $F^+1 \approx 1$.

Visbal and Gaitonde [12] deployed asymmetric DBD plasma actuators on the apex of a 75 deg swept delta wing to control the vortical flows by numerical simulation. The actuator was placed at $x/c = 0.08$ and extended in a spanwise direction. The strength of the plasma actuator was chosen to be $D_c = 2400$. The changes near the apex of the wing, induced by the plasma, resulted in significant downstream displacements of the vortex breakdown location. This effect could be potentially beneficial for roll control authority at high angles of attack. Following actuation, the unsteady shear layer evolved into a steady pattern, characterized by stationary helical subvortices. The origin of these steady substructures appeared to be linked to the increase in axial velocity within the secondary vortex, induced by the momentum injection of the actuator.

In this technical note, the configurations of the plasma actuator on the delta wing, similar to that used in Visbal and Gaitonde's simulation [12], are used. The plasma actuators are mounted in different chordwise locations on the leeward side of the delta wing. The effect of the location of the plasma actuator on the aerodynamic performance of the delta wing is studied by the balanced force measurement in the wind tunnel. At last, the smoke wire visualization is used to present the flow structure variation induced by the plasma actuator.

II. Experimental Setup

The experiment is conducted in the D1 open-circuit low-speed wind tunnel of the Beijing University of Aeronautics and Astronautics. The test section of the tunnel is nominally 0.76 m high, 1.02 m wide (with a quasi-elliptical cross section), and 1.5 m long. The turbulence intensity of the freestream velocity is about 1%. The model used in the experiment is constructed from epoxy resin. The delta wing has a 75 deg swept leading edge with a chord length of $c = 250$ mm and a thickness of $h = 10$ mm. There are six pair of electrodes deployed on the leeward surface of the delta wing. Figure 1 and Table 1 give the details of the locations about the plasma actuators. Each plasma actuator is made from the two electrodes, which are separated by a 1-mm-thick dielectric. The anode is exposed on the atmosphere environment with a width of 2 mm, and the cathode is encapsulated in the delta wing with a width of 6 mm. The frequency of the power source is 20 kHz, and the input voltage is 5.4 kV. The estimated strength of the plasma actuator in the experiment, according to Visbal's definition, is $Dc = 1.133$. For the fourth electrode, E4 has been destroyed by high voltage during the experiment preparation, the result in this note does not conclude the data for this case.

The time-averaged lift and drag forces of the delta wing are measured by a six-component internal strain gauge balance. The delta wing model is sting mounted from the trailing edge, in the wind tunnel. The range of the angle of attack varies from 0 to 42 deg. The overall uncertainty in both the lift and the drag measurements was estimated at 1%, by repeating the force measurement of the delta wing several times. In the smoke wire visualization, a fine stainless steel wire is placed in the vertical symmetrical plane of the delta wing and is about 3 mm upstream from the delta wing apex. The freestream

Received 5 August 2008; revision received 27 September 2009; accepted for publication 27 September 2009. Copyright © 2009 by the American Institute of Aeronautics and Astronautics, Inc. All rights reserved. Copies of this paper may be made for personal or internal use, on condition that the copier pay the $10.00 per-copy fee to the Copyright Clearance Center, Inc., 222 Rosewood Drive, Danvers, MA 01923; include the code 0001-1452/10 and $10.00 in correspondence with the CCC.

*Associate Professor, Institute of Fluid Mechanics; Key Laboratory of Fluid Mechanics (Ministry of Education); pfzhang@buaa.edu.cn.
†Professor, Institute of Fluid Mechanics; jjwang@buaa.edu.cn. Member AIAA.
‡Ph.D Candidate, Institute of Fluid Mechanics; fblueair@163.com.
§Graduate Student, Institute of Fluid Mechanics.

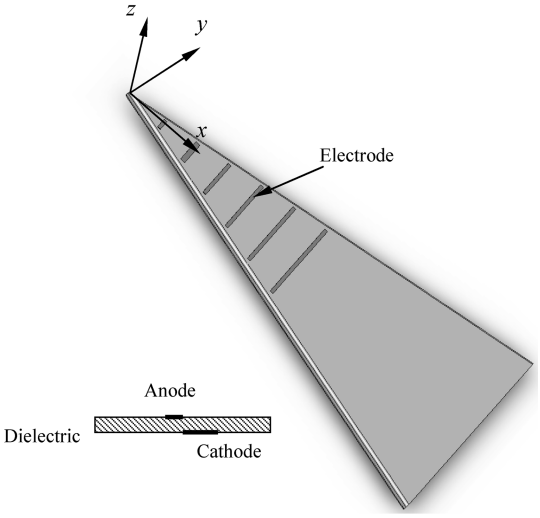

Fig. 1 The sketch of the delta wing model and the electrodes.

incoming flow velocity in the force measurement experiment is 16.5 m/s, which results in the Reynolds number based on the chord of the delta wing $Re = 2.82 \times 10^5$. The corresponding freestream velocity and the Reynolds number in the smoke wire visualization are 5.35 m/s and 9.08×10^4, respectively.

III. Results and Discussion

The lift coefficients of the delta wing, with respect to the angle of attack excited by different plasma actuators, are presented in Fig. 2. The data of the cleaning delta wing without the plasma actuator are also concluded as the baseline case. With electrode E1 discharged, which is at the same location relative to the delta wing as that in Visbal and Gaitonde's numerical simulation [12], there is no obvious lift enhancement on the delta wing at low and moderate angles of attack, and only limited lift increase appears in the poststall region ($\alpha > 32$ deg). This difference between the experiment and the previous numerical simulation is possibly caused by the different strength of the discharge electric field. In Visbal and Gaitonde's numerical simulation [12], the strength of the plasma actuator is $Dc = 2400$, which is only $Dc = 1.133$ in the present experiment. Hence, in their study, the plasma actuator can add enough momentum to the vortex core and increase the axial velocity in the leading-edge vortex apparently, which results in the breakdown location of the leading-edge vortex being shifted downstream from about $x_b/c = 0.6$ (estimated from Figs. 19–21 in [12]) to downstream of the trailing edge. But in our experiment, the location of the leading-edge vortex breakdown point has no obvious change by flow visualization. As the downstream electrodes (E2, E3, and E5) ignited, the effect of the plasma actuator for the delta wing lift enhancement is noticeable. The lift of the delta wing increases with the electrode downstream movement, and the length increases. The optimum value appears for electrode E5, and the maximum lift increases by 10.6%. The other feature is that the lift increase extent, caused by the plasma actuator on the delta wing, increases with the angle-of-attack increase. This explained that the plasma actuator influences the aerodynamic characteristics of the delta wing by interacting with the leading-edge vortex. With the plasma actuator inducement, a wall jet is formed to provide additional momentum to the leading-edge vortex, preserving the jetlike profile of the vortex core. Therefore, the vortex breakdown is pushed father downstream, and the lift of the delta wing is enhanced. This mechanism is the same as the leading-edge vortex

Table 1 The position and scale of the electrodes

Electrodes	E1	E2	E3	E4	E5	E6
Position (from the apex)	8%c	16%c	24%c	32%c	40%c	48%c
Length, mm	10	21	32	42	53	64

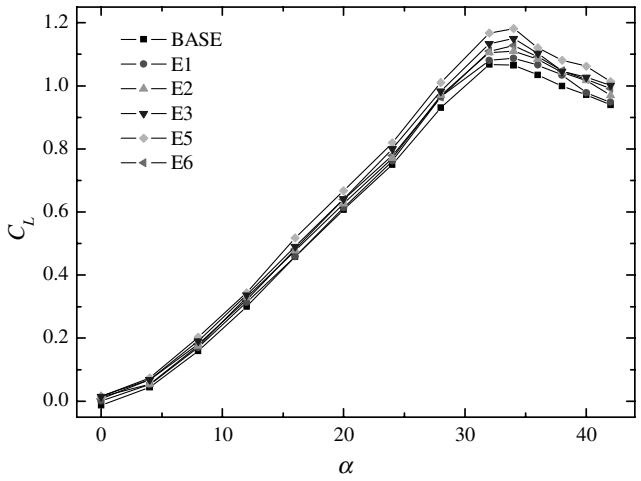

Fig. 2 Lift coefficients for the base case and with the plasma actuator.

breakdown control along the core, blowing over the delta wing [13,14]. With the last electrode E6 actuated, the lift increase is not as much as that with electrode E5, although the length of electrode E6 is larger. This indicates that there exists an optimum location for the plasma actuator, induced along the core injection to control the leading-edge vortex. Gutmark and Guillot [14] also concluded that the leading-edge vortex should be allowed to develop to a certain level before the control jet is injected into its core. For the 75 deg swept delta wing at a moderate Reynolds number in this note, the optimum location for the plasma actuator is about 40%c.

In addition to the lift coefficient, the plasma actuator also changes the drag coefficient of the delta wing. Figure 3 plots the drag coefficient vs the angle of attack of the delta wing, induced by a different plasma actuator. With electrode E1 actuated, the drag coefficients of the delta wing have much increase in the whole range of the angle of attack. As electrodes E2 or E3 work on, the drag coefficients of the delta wing decrease when compared with that for electrode E1, but they are still a little larger than that of the cleaning delta wing. For the last two electrodes (E5 and E6), the drag coefficients of the delta wing with the plasma actuator are very close to that of the cleaning delta wing at most angles of attack and even less than that of the base case at a small angle of attack.

Based on the variation of the lift and drag coefficients discussed previously, Fig. 4 presents the lift-to-drag ratio, with respect to the angle of attack, with different electrodes actuated. Because the drag coefficient of the delta wing (with electrode E1 actuated) has large increase, the lift-to-drag ratio for this case decreases a lot in a large range of the angle of attack (4 deg $< \alpha <$ 28 deg). With electrodes E2 or E3 actuated, although the lift coefficient increases when compared with the baseline case, the lift-to-drag ratio is very close to that of the

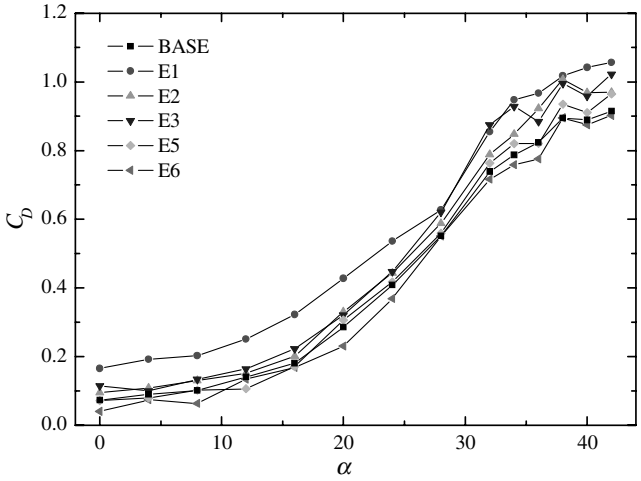

Fig. 3 Drag coefficients for the base case and with the plasma actuator.

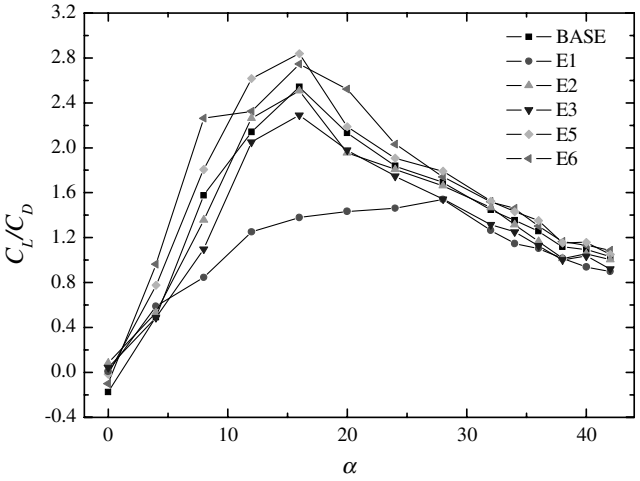

Fig. 4 Lift-to-drag ratio for the base case and with the plasma actuator.

cleaning delta wing, for the drag coefficient in this case also increases (seen in Fig. 3). The best lift-to-drag ratio performance appears with electrodes E5 or E6, which is due to the lift enhancement in the whole range of the angle of attack and the drag decrease at a low angle of attack. With electrode E5 actuated, the maximum lift-to-drag ratio increases by 11.7% when compared with that of the clean delta wing.

To explain the force variation of the delta wing with the plasma actuator, Fig. 5 gives the smoke wire visualization photos of the delta wing with electrode E5 worked on/off to compare. The attack angle of the delta wing in Fig. 5 is 38 deg, which is in the poststall region for the 75 deg swept delta wing. The photos present the flow structures on the leeward side of the delta wing. According to Lowson and Riley's method [15], the leading-edge vortex of the delta wing will entrain the smoke to visualize itself (except at the center where the smoke particles are centrifuged out), producing a dark core. Therefore, the leading-edge vortex breakdown point can be judged as the chordwise location where the dark core first begins to expand. This feature is obvious in Fig. 5 in the present study. Upstream of the leading-edge vortex breakdown point, the smoke wire rolls regularly around the vortex core, and there is a thin dark core behind the smoke streak lines. As the leading-edge vortex begins to breakdown, the vortex core suddenly expands, and a turbulent region full of smoke particles appears. By using this judgment, it is obvious that the leading-edge vortex breakdown point with the plasma actuator in Fig. 5b is pushed down when compared with that without the plasma actuator in Fig. 5a. By averaging the chordwise location for the leading-edge vortex breakdown point, the data indicate that the vortex breakdown point is delayed from $0.68c$ to $0.76c$, with electrode E5 actuated, which results in the lift and lift-to-drag ratio performance enhancements of the delta wing.

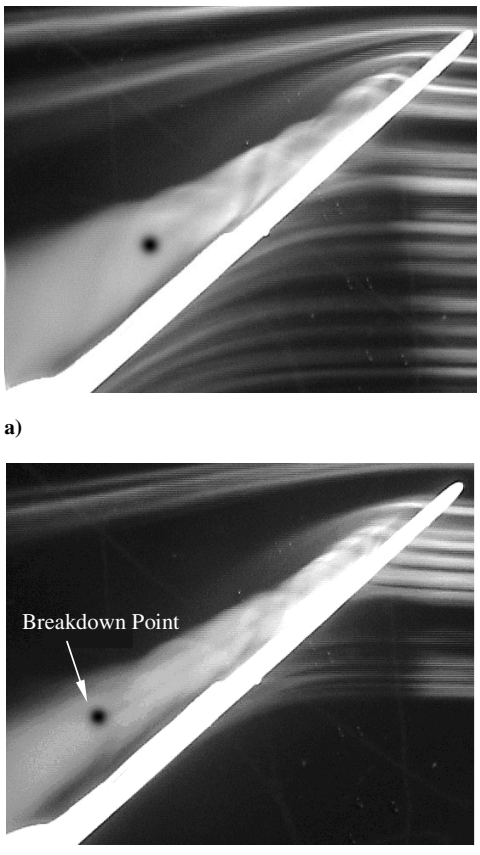

a)

b)

Fig. 5 The leading-edge vortex breakdown point a) for the base case and b) with electrode E5 actuated in the poststall region at $\alpha = 38$ deg.

IV. Conclusions

The force measurement and the smoke wire visualization experiments are carried out in the wind tunnel to investigate the effect of the plasma actuator in different chordwise locations on the aerodynamic characteristics of a 75 deg swept delta wing. The plasma actuators are mounted at the leeward side of the delta wing and induce a wall jet to downstream. The results demonstrate that the plasma actuator can improve the aerodynamic performance of the highly swept delta wing at the proper chordwise location. The optimum location of the plasma actuator for the 75 deg swept flat plate delta wing at a moderate Reynolds number ($Re = 2.82 \times 10^5$) in the present study is about $40\%c$. The maximum lift and lift-to-drag ratios are increased by 10.6% and 11.7%, when compared with that of the cleaning delta wing, respectively.

Acknowledgments

The present research was supported by the National Natural Science Foundation of China under grant No. 10872021, the Research Fund for the Doctoral Program of Higher Education under grant No. 200800061040, and the Aviation Creative Foundation of China under grant No. 07A51001.

References

[1] Corke, T. C., Post, M. L., and Orlov, D. M., "SDBD Plasma Enhanced Aerodynamics: Concepts, Optimization And Applications," *Progress in Aerospace Sciences*, Vol. 43, Nos. 7–8, 2007, pp. 193–217. doi:10.1016/j.paerosci.2007.06.001

[2] Greenblatt, D., Kastantin, Y., Nayeri, C. N., and Paschereit, C. O., "Delta Wing Flow Control Using Dielectric Barrier Discharge Actuators," *AIAA Journal*, Vol. 46, No. 6, 2008, pp. 1554–1560. doi:10.2514/1.33808

[3] Suchomel, C., Van, W. D., and Risha, D., "Perspectives on Cataloguing Plasma Technologies Applied to Aeronautical Sciences," AIAA Paper 2003-3852, 2003.

[4] Roth, J. R., Tsai, P. P., Liu, C., Laroussi, M., and Spence, P. D., The Univ. of Tennessee Research Corp., Knoxville, TN, U.S. Patent Application for a "One Atmosphere Uniform Glow Discharge Plasma," Docket No. 5,414,324, filed 09 May 1995.

[5] Moreau, E., "Airflow Control by Non-Thermal Plasma Actuators," *Journal of Physics D: Applied Physics*, Vol. 40, No. 3, 2007, pp. 605–636. doi:10.1088/0022-3727/40/3/S01

[6] Jukes, T. N., Choi, K. S., and Johnson, G. A., "Turbulent Boundary-Layer Control for Drag Reduction Using Surface Plasma," AIAA Paper 2004-2216, 2004.

[7] Post, M. L., and Corke, T. C., "Separation Control on High Angle of Attack Airfoil Using Plasma Actuators," *AIAA Journal*, Vol. 42, No. 11, 2004, pp. 2177–2184. doi:10.2514/1.2929

[8] Zhang, P. F., Liu, A. B., and Wang, J. J., "Aerodynamic Modification of NACA 0012 Airfoil by Trailing Edge Plasma Gurney Flap," *AIAA Journal*, Vol. 47, No. 10, 2009, pp. 2467–2474. doi:10.2514/1.43379

[9] Post, M. L., and Corke, T. C., "Separation Control Using Plasma Actuators: Dynamic Stall Vortex Control on Oscillating Airfoil," *AIAA*

Journal, Vol. 44, No. 12, 2006, pp. 3125–3135.
doi:10.2514/1.22716

[10] Patel, M. P., Ng, T. T., Vasudevan, S., Corke, T. C., and He, C., "Plasma Actuators for Hingeless Aerodynamic Control of an Unmanned Air Vehicle," *Journal of Aircraft*, Vol. 44, No. 4, 2007, pp. 1264–1274.
doi:10.2514/1.25368

[11] Nelson, R. C., Corke, T. C., Otham, H., Matsuno, T., Patel, M. P., and Ng, T. T., "Modification of the Flow Structure Over a UAV Wing for Roll Control," AIAA Paper 2007-0884, 2007.

[12] Visbal, M. R., and Gaitonde, D. V., "Control of Vortical Flows Using Simulated Plasma Actuators," AIAA Paper 2006-505, 2006.

[13] Gursul, I., Wang, Z., and Vardaki, E., "Review of Flow Control Mechanisms of Leading-Edge Vortices," AIAA Paper 2006-3508, 2006.

[14] Gutmark, E. J., and Guillot, S. A., "Control of Vortex Breakdown Over Highly Swept Wings," *AIAA Journal*, Vol. 43, No. 9, 2005, pp. 2065–2069.
doi:10.2514/1.11326

[15] Lowson, M. V., and Riley, A. J., "Vortex Breakdown Control by Delta Wing Geometry," *Journal of Aircraft*, Vol. 32, No. 4, 1995, pp. 832–838.
doi:10.2514/3.46798

J. Gore
Associate Editor